Canine Model of Terminal Arterial Aneurysm

Virgil B. Graves,[1] Arvind Ahuja,[1,2] Charles M. Strother,[1] and Al H. Rappe[1]

Summary: A canine model of terminal aneurysms using a venous pouch surgical technique is described. This model mimics the anatomy and hemodynamics of some types of carotid and basilar tip aneurysms. This technique produces aneurysms 15 × 21 mm in size. The aneurysms have been used to investigate the hemodynamics and treatment of terminal aneurysms.

Index terms: Aneurysm, arteriovenous; Interventional neuroradiology, models; Animal studies

The natural history of intracranial aneurysms is directly related to the effects of hemodynamic forces (1–5). The hemodynamics of aneurysms have been studied with mathematical modeling, computer simulation, glass models, and, recently, in vivo models (6–11). The development of in vivo models is critical for understanding the hemodynamic forces present in aneurysms and for evaluating therapeutic endovascular devices and techniques (7, 12). Three types of aneurysms (lateral, bifurcation, and terminal) have been described, each with distinctly different anatomic configurations and hemodynamic flow characteristics (7, 11). In vivo models of lateral and bifurcation aneurysms have been described (5, 10, 12–14, 16). These models do not mimic the geometry of terminal aneurysms. We have developed a reproducible terminal aneurysm model in the dog; this model closely mimics the anatomic configuration of terminal aneurysms, and provides an in vivo model to study the hemodynamics and endovascular treatment of this type of aneurysm.

Materials and Method

Six mongrel male dogs weighing approximately 20 kg were used. All surgical procedures were performed under sterile conditions. General anesthesia was induced with intravenous 5% pentothal (1 mL/5 lbs) followed by endotracheal intubation, and was maintained with 1.0% to 2.0% halothane and 100% oxygen. The dogs were not systemically heparinized.

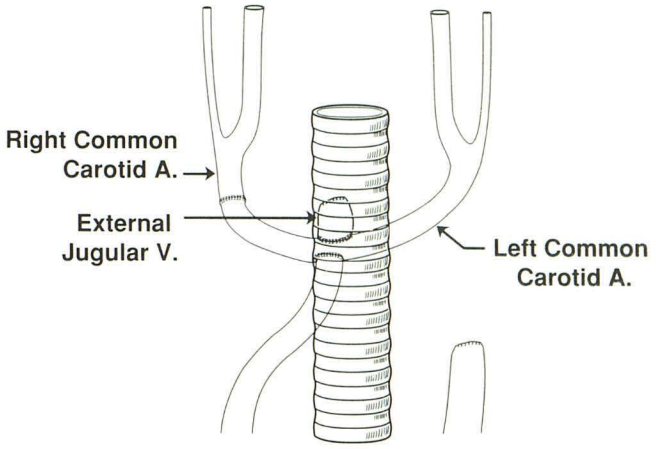

Fig. 1. A left to right carotid artery end to end anastomosis forming a U. The venous pouch graft is anastomosis on the superior surface of the U. The proximal right carotid artery is anastomosis to bottom of the U.

Bilateral 8-cm incisions were made lateral to the sternohyoidus muscle in the neck to expose the right and left common carotid arteries. The external jugular vein on one side was isolated and ligated proximally and distally, and a 3-cm segment of vein was excised and placed in heparinized saline (2000 U heparin/20 cc normal saline). The left common carotid artery was ligated proximally and a temporary vascular clamp was placed as far distal as possible. The artery was then divided just above the proximal ligature. A tunnel was made behind the trachea and the distal segment of the left common carotid artery was passed through it to the right side of the neck. The right common carotid artery was then clamped at the proximal and distal extent of the exposure with temporary vascular clamps and was divided 2 cm proximal to the distal clamp. An end to end anastomosis was made between the distal segments of the left and right common carotid arteries forming a U-shaped tube (Fig. 1). A 5-mm Hancock vascular punch was then used to make a circular opening on both the superior and inferior surfaces at the base of the U. The

Received March 9, 1992; revision requested July 27, received August 27, and accepted October 1.

[1] Department of Radiology, University of Wisconsin Clinical Science Center, 600 North Highland Avenue, Madison, WI 53792-3252. Address reprint requests to V. B. Graves, MD.

[2] Department of Neurosurgery, State University of New York at Buffalo, Buffalo, NY 14203-1194.

AJNR 14:801–803, Jul/Aug 1993 0195-6108/93/1404–0801

proximal right common carotid artery was then anastomosed end to side at the undersurface of the U and a 2.5- to 3-cm segment of the excised jugular vein was anastomosed end to side on its superior surface. The distal free end of the vein was oversown. A Prolene suture 7-0, tapered needle (Ethicon, Inc., Somerville, NJ) was used for all anastomoses. The vascular clamps were removed. The animals were allowed to recuperate for at least 2 weeks prior to further study. Serial transfemoral carotid angiograms were performed on each dog, at varying times between 9 and 17 weeks after aneurysm construction, to evaluate the patency and size of the aneurysm.

Results

Experimental aneurysms were created successfully in all six dogs. Approximately 3 hours of surgical time were needed to construct each aneurysm. There were no neurologic complications or deaths. The animals were observed for an average of 13 weeks (9–17 wks). The patency of the aneurysms was 100%. This method of construction produced aneurysms with an average width of 15 mm and height of 21 mm (Fig. 2A). Over the period of observation, the aneurysms increased in size by an average of 5 mm in width and 2 mm in height; they also became more saccular in shape (Fig. 2B). Aneurysm growth has been noted previously in lateral and bifurcation aneurysm models constructed using the venous pouch technique (12, 15, 17). Following an observation period of 9 to 17 weeks, the aneurysms were used to study their hemodynamics and to evaluate endovascular devices and treatment techniques.

The hemodynamic characteristics of these terminal aneurysms were distinctly different from those of a lateral aneurysm canine model. Circulation within these aneurysms was rapid and hyperdynamic, with no angiographic evidence of stasis or vortex formation (11).

Discussion

The pathophysiology of cerebral saccular aneurysm formation, growth, thrombosis, and rupture is influenced by hemodynamic forces (1–3, 18). Hemodynamic forces also have a significant influence on devices used for the endovascular treatment of aneurysms (7). The geometrical relationship of an aneurysm to its parent artery and branches is an important determinant of the hemodynamic stresses imparted to aneurysms and endovascular devices (4, 5, 19). It is critical that these hemodynamic forces be understood for the successful treatment of an aneurysm.

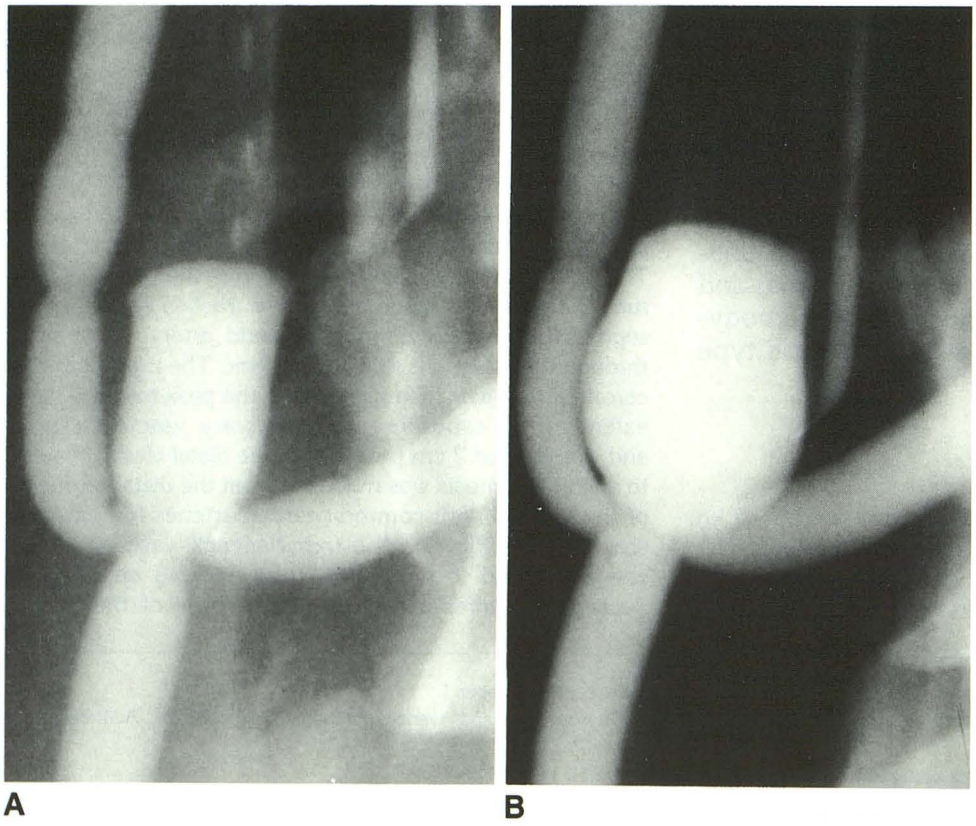

Fig. 2. *A*, Transfemoral right carotid angiogram 1 week after surgery. Size of aneurysm: 10 mm in width and 19 mm in height.

B, Repeat angiogram 10 weeks after surgery. Size of aneurysm: 15 mm in width and 22 mm in height. Note the increase in size and the more saccular shape of the aneurysm.

This aneurysm model has hemodynamic characteristics distinctly different from those of a lateral aneurysm model (11). The circulation within these aneurysms is hyperdynamic, with no evidence of stasis. This hyperdynamic flow in terminal aneurysm models caused coils to behave differently than they do in lateral aneurysms. The changes of coil compaction and migration occurred in both terminal and lateral aneurysm models; however, these changes occurred more rapidly and to a greater degree in the terminal aneurysm model.

The terminal aneurysm model with its unique hemodynamics has allowed us to make comparisons of the flow characteristics of three different anatomic aneurysm configurations (11). It also provides an in vivo model to observe and develop endovascular devices, teach endovascular techniques, and study aneurysm hemodynamics.

References

1. Ferguson GG. Physical factors in the initiation, growth, and rupture of human intracranial saccular aneurysms. *J Neurosurg* 1972;37:666–677
2. Sekhar LN, Heros RC. Origin, growth, and rupture of saccular aneurysms: a review. *Neurosurgery* 1981;8:248–260
3. Stehbens WE. Etiology of intracranial aneurysms. *J Neurosurg* 1989;70:823–831
4. Steiger HJ, Poll A, Liepsch D, Reulen HJ. Haemodynamic stress in lateral saccular aneurysms: an experimental study. *Acta Neurochir (Wein)* 1987;86:98–109
5. Steiger HJ, Liepsch DW, Poll A, Reulen HJ. Hemodynamic stress in terminal saccular aneurysms: a laser-Doppler study. *Heart Vessels* 1988;4:162–169
6. German W, Black SPW. Intra-aneurysmal hemodynamics turbulence. *Trans Am Neurol Assoc* 1954;74:163–165
7. Graves VB, Strother CM, Partington CR, Rappe AH. Flow dynamics of lateral carotid artery aneurysms and their effects on coils and balloons: an experimental study in dogs. *AJNR: Am J Neuroradiol* 1992;13:189–196
8. Perktold K, Gruber K, Kenner T, Florian H. Circulation of pulsatile flow and particle paths in aneurysm-model. *Basic Res Cardiol* 1984;79:253–261
9. Perktold K. On paths of fluid particles in axisymmetrical aneurysm. *J Biomech* 1987;20:311–317
10. Stehbens WE. Experimental production of aneurysms by microvascular surgery in rabbits. *Vasc Surg* 1973;7:165–175
11. Strother CM, Graves VB. Aneurysm hemodynamics: an experimental study. *AJNR: Am J Neuroradiol* 1992;13:1089–1095
12. Graves VB, Partington CR, Rufenacht DA, Rappe AH, Strother CM. Treatment of carotid artery aneurysms with platinum coils: an experimental study in dogs. *AJNR: Am J Neuroradiol* 1990;11:249–252
13. Forrest MD, O'Reilly GV. Production of experimental aneurysms at a surgically created arterial bifurcation. *AJNR: Am J Neuroradiol* 1989;10:400–402
14. German WJ, Black SPW. Experimental production of carotid aneurysm. *N Engl J Med* 1954;250:104–106
15. Nishikawa M, Yonekawa Y, Matsuda I. Experimental aneurysms. *Surg Neurol* 1976;5:15–18
16. Young PH, Yasargil MG. Experimental carotid artery aneurysms in rats: a new model for microsurgical practice. *J Microsurg* 1982;3:135–146
17. Moritake K, Handa H, Hayashi K, Sato M. Experimental studies of intracranial aneurysm (a preliminary report). Some biomechanical considerations on the wall structures of intracranial aneurysms and experimentally produced aneurysms. *Neurol Surg (Tokyo)* 1973;1:115–123
18. Ferguson GG. Direct measurement of mean and pulsatile blood pressure at operation in human intracranial saccular aneurysms *JNS* 1972;36:560–563
19. Steiger HJ, Reulen HJ. Low frequency flow fluctuations in saccular aneurysms. *Acta Neurochir (Wien)* 1986;83:131–137